J Mater Sci (2007) 42:9392–9401
DOI 10.1007/s10853-007-1813-5

Gas permeation properties of polyamide membrane prepared by interfacial polymerization

S. Sridhar · B. Smitha · Satyajai Mayor · B. Prathab · T. M. Aminabhavi

Received: 29 September 2006 / Accepted: 30 April 2007 / Published online: 20 July 2007

Abstract Interfacial polymerization technique has been widely employed to prepare reverse osmosis (RO) and nanofiltration (NF) membranes. The present study explores the possibility of preparing a polyamide membrane by interfacial polymerization and its utilization for the separation of CO_2 and H_2S from CH_4. A novel ultraporous substrate of polysulfone (PSF) was prepared by phase inversion technique from a solution containing 18% PSF and 4% propionic acid in dimethyl formamide (DMF) solvent. Thin film composite (TFC) polyamide membrane was synthesized on PSF substrate from the reaction between *meta*-phenylene diamine in an aqueous media and isophthaloyl chloride in hexane. The membrane prepared was characterized by Fourier transform infrared spectroscopy (FTIR), X-ray diffraction (XRD), differential scanning calorimetry (DSC) and scanning electron microscopy (SEM) to study intermolecular interactions, crystallinity, thermal stability and surface morphology, respectively. Gas permeabilities of pure CO_2, H_2S, CH_4, O_2, and N_2 gases were measured using the indigenously built permeation cell incorporated into a high-pressure gas separation manifold. At the feed pressure of 1 MPa, the membrane exhibited permeances of 15.2 GPU for CO_2 and 51.6 GPU for H_2S with selectivities of 14.4 and 49.1 for CO_2/CH_4 and H_2S/CH_4 systems, respectively. The observed N_2 permeance of 0.95 GPU was close to that of CH_4. The corresponding O_2 permeance was 5.13 GPU with a reasonably high O_2/N_2 selectivity of 5.4. The effect of feed pressure on polyamide membrane performance was examined. Further, molecular dynamics (MD) simulations were employed to compute the cohesive energy density (CED), solubility parameter (δ) and sorption of CO_2, H_2S, CH_4, O_2, and N_2 gases in polyamide membrane to corroborate theoretical study with experimentally determined gas transport properties.

S. Sridhar · B. Prathab · T. M. Aminabhavi (✉)
Membrane Separations Division, Center of Excellence in Polymer Science, Karnatak University, Dharwad 580 003, India
e-mail: aminabhavi@yahoo.com

S. Sridhar · B. Smitha
Membrane Separations Group, Indian Institute of Chemical Technology, Hyderabad 500 007, India

S. Mayor
Permionics Membranes Pvt. Ltd., Vadodara 390 016, India

Introduction

Interfacial polymerization has been widely employed to fabricate commercial membranes for applications in reverse osmosis [1, 2] and nanofiltration [3–6]. Recently, Kim et al. [7] reported the preparation of thin film composite (TFC) polyimide membrane for the pervaporation (PV) separation of water from ethanol. The advantage of membranes prepared by interfacial polymerization is that the active skin layer could be as thin as 0.1–1.0 μm, which would allow maximum flux with reasonably high impurity rejection. Other factors that make them commercially viable are their defect-free nature and ease in scaling-up to spiral wound or hollow fiber elements. In general, such membranes are prepared by saturating an ultraporous support with a water-based diamine reagent such as *meta*-phenylene diamine or piperazine followed by a reaction in an organic media containing a di-acid chloride such as isophthaloyl chloride or trimesoyl chloride [8–12]. The pore structure in these membranes is generally far too open (0.5×10^{-10} to 20×10^{-10} m) to enable the separation of gaseous mixtures like CO_2/CH_4 or O_2/N_2. The majority of gas separation membranes are non-porous barriers based on

glassy polymers such as polysulfone, polycarbonate, polyimide etc., prepared in the form of flat sheets (spiral wound) or hollow fibers using the phase inversion technique or dip-coating method [13].

Sour natural gas contains CO_2 (5–7 mol%), H_2S (1500–2000 ppm) and H_2O as the major impurities, which cause corrosion and lowering of the calorific value [14]. The present method employed to remove CO_2 and H_2S involves the absorption in amine solvents, monoethanolamine (MEA) and diethanolamine (DEA) [15, 16]. These techniques are energy-intensive, polluting and would pose problems related to solvent regeneration. Therefore, an economical, safe and eco-friendly alternative separation method would be highly demanding. In this context, separation based on membranes is expected to play a significant role in chemical industries due to comparatively lower capital and operating costs, high recovery rates, besides simpler and cleaner modes of operation involved [17]. Particularly, membrane-based gas separation is quite attractive for the purification of natural gas mixtures, provided suitable polymeric membranes are developed, which would offer high CO_2 flux as well as good separation characteristics for CO_2/CH_4 and H_2S/CH_4 systems [18]. Enrichment of O_2 from air is another significant separation problem that requires an alternative process to cryogenic distillation, which involves extreme conditions and high operating costs [17].

Aromatic polyamide membranes have been investigated in the past for their gas transport properties [19–23]. Espeso et al. [19] reported reasonably high CO_2/CH_4 selectivities in the range 18.3–27.7 and O_2/N_2 selectivities of 5.2–6.6 with different aromatic polyamide membranes. Ekiner and Vassilatos [20] worked on polyaramide hollow fibers for H_2/CH_4 separation. Researchers also attempted preparation of interfacial polyamide for gas separation [21, 22]. Petersen and Peinemann [21] achieved low selectivities of 5.5 and 2.2 for CO_2/CH_4 and O_2/N_2 systems, which improved to 8.6 and 3.4, respectively, after a silicone-coating step that plugged inherent defects in the polyamide layer. However, aromatic polyamides have not attracted special attention as membrane forming materials as they do not melt and are poorly soluble in highly polar organic solvents. There are inherent structural elements, which are responsible for these drawbacks such as high degree of chain rigidity, which accounts for high cohesive energy density and molecular packing [19]. The present study explores the possibility of tailoring the aromatic polyamide membrane by interfacial polymerization technique to improve flux and suit gas separation applications. The gas separation results were further supported by molecular modeling (MM) approaches, leading to the understanding of polymer/gas interfacial energies. The gas sorption phenomena were studied through MD simulations to estimate the interaction energy of CO_2, H_2S, CH_4, O_2, and N_2 molecules with polyamide membrane.

Experimental

Materials

Meta-phenylene diamine and isophthaloyl chloride of 99.5% purity were supplied by Aldrich Chemical Co., Milwaukee, WI, USA. Dimethyl formamide, hexane, and propionic acid of ≥99% purity were all purchased from Loba Chemie, Mumbai, India. Polysulfone (Udel bisphenol A polysulfone P1800, M_n = 35,000) was supplied by Permionics Membranes Pvt. Ltd., Vadodara, India. All the gases used in this study were supplied by Inox Air Products, Mumbai, India.

Membrane preparation

The most critical part in the preparation of a TFC membrane is the surface morphology of the substrate. Tightness of the ultraporous substrate determines the pore structure of the skin layer that will be formed during interfacial polymerization. Polysulfone substrate was prepared by phase inversion technique using 18% (w/v) solution of the polymer in DMF solvent, which contained 4% propionic acid as the surfactant additive. This particular additive is expected to cause shrinkage of the pores during the membrane formation [24]. The solution was cast onto a non-woven polyester membrane support fabric of 100 μm thickness, which was fastened onto a glass plate. The cast film was gelled in an ice-cold water bath for 5 min. The molecular weight cut off (MWCO) of polysulfone substrate was found to be approximately 5000 Daltons using aqueous solutions containing 2000 ppm of polyethylene glycol (PEG) of different molecular weights. The support was found to reject 80–85% of PEG of 5000 molecular weight at 350 kPa pressure.

Polysulfone support was initially saturated in a water bath containing 2% (w/v) *meta*-phenylene diamine (MPD) for 2 min. Excess water was drained off from the polysulfone support before immersion in an organic bath consisting of 0.5% isophthaloyl chloride (IsoCl) in hexane for 30 s. The resultant TFC membrane was heated in an oven at 130 °C for 50 min. Figure 1 represents the reaction scheme between MPD and IsoCl, resulting in the formation of interfacial polyamide membrane.

Permeation studies

A schematic diagram of the high-pressure gas separation manifold used in permeation studies is given in Fig. 2. A permeation cell of stainless steel (SS 316), having an

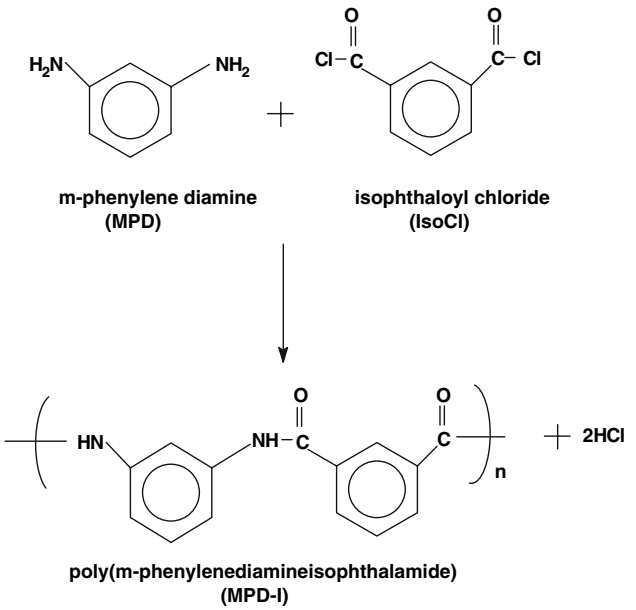

Fig. 1 Structural representation of reaction mechanism between *m*-phenylene diamine (MPD) and isophthaloyl chloride (IsoCl) resulting in the formation of interfacial polyamide

effective area of 0.0042 m^2, was designed and fabricated indigenously; it is displayed in Fig. 3(a, b).

Design of permeation cell

The cell consisted of: (i) bottom plate, which housed the perforated plate and membrane, (ii) top plate, which had the provision for feed distribution across the membrane, and (iii) locking ring to fasten the top plate onto the bottom plate for a leak proof arrangement. A step of 15 mm depth was provided in the bottom plate for insertion of a perforated plate. The membrane was fixed on a circularly perforated plate of 84 mm outer diameter (OD) by applying vacuum grease at the edges. An O-ring made of neoprene rubber was placed on the membrane after which, the top plate was inserted into the bottom plate. Figure 3(a) shows two internally threaded ports, each on the surface of a top plate, for feed inlet and at downstream surface of the bottom plate for permeate outlet. Adapters with one side having 3 mm external threading and another side suitable for 6 mm nut and ferrule fittings were provided for connecting the permeation cell to the manifold. A thin circular copper tube having perforations for slow and uniform feed introduction (not shown in the figure) is provided at the inside surface of the top plate to minimize the concentration polarization, while the feed flows through the cell. Aligning pins of 2 mm OD were used during the insertion to ensure that the membrane does not undergo movement during the tightening action of the internally threaded locking ring, which presses the top plate onto the O-ring atop the membrane in the bottom plate. The overall thickness of the metal surrounding the membrane enclosure from any direction in this leak-proof arrangement is 26.4 mm, which was sufficient to withstand the working pressure of 6.0 MPa. A photograph of the actual cell used in the present studies is depicted in Fig. 3(b).

Feed and permeate lines in the manifold were made of 6 mm OD stainless steel piping connected together by means of compression fittings. The vacuum line consisted of a network of high-vacuum rubber-glass valve connections capable of giving a pressure as low as 6.7 Pa. Feed and permeate lines in the manifold were made of 6 mm stainless steel piping connected together by means of compression fittings. The carrier gas cylinder was only used to determine the permeation of methane and nitrogen at lower pressures (1 MPa) by the continuous flow method, which is described in detail elsewhere along with the

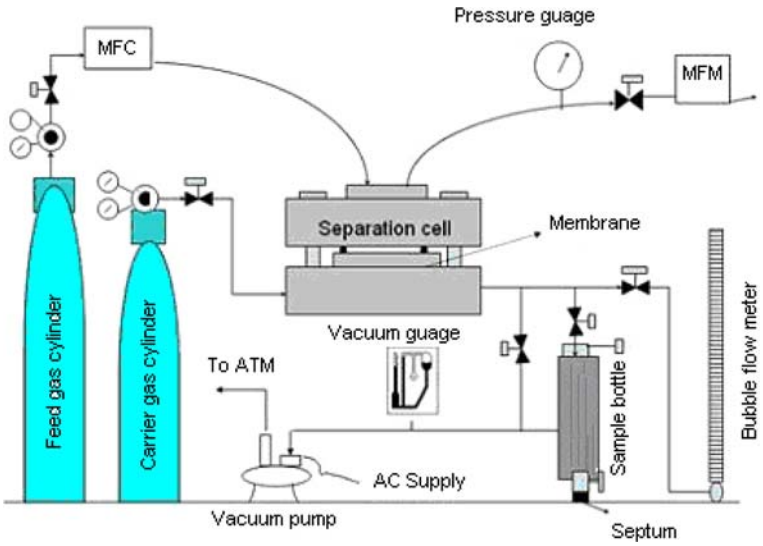

Fig. 2 Experimental manifold for gas permeability measurement

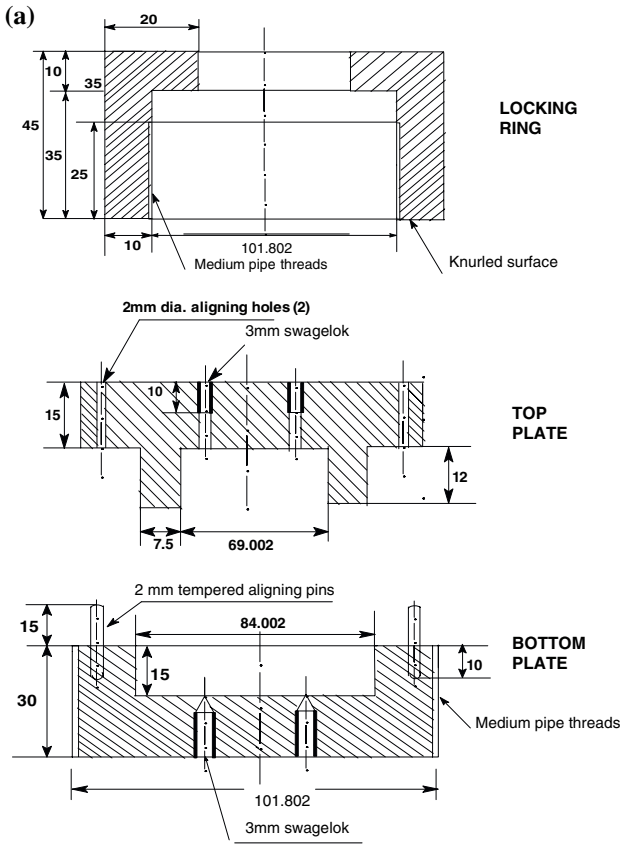

Fig. 3 (**a**) Design of gas permeability cell. (**b**) Photograph of gas permeability cell components

requisite analytical procedure [25]. For all other experiments, permeate rate was sufficient enough for direct measurement of its flow through a soap bubble meter, which means that only the valve leading to the flow indicator was kept open, whereas all other needle valves in the permeate line were closed. Back permeation of H_2 carrier gas was minimized by collecting the permeate mixture at a pressure less than 50 kPa. Experiments were performed at the ambient temperature (30 °C) and repeated five times to ensure reproducibility of data, which were reported to an accuracy of ±2% of standard errors. Instead of permeation coefficient, permeance (k) was reported throughout this work, since it was difficult to accurately determine the exact thickness of the polyamide skin layer formed in the TFC membrane as well as its extent of penetration into the polysulfone support. The permeance was calculated as:

$$k = \frac{Q}{tA(P1 - P2)} \tag{1}$$

where Q is volume of the permeated gas [(m^3 (STP))]; t, the permeation time (s); A, the effective membrane area (m^2) for gas permeation, $P1$ and $P2$ are feed side and permeate side partial pressures (Pa), respectively. The unit of permeance is denoted as GPU [1 GPU = 7.5×10^{-12} $m^3/(m^2.s.Pa)$]. Selectivity was determined as the ratio of permeances of CO_2 or H_2S with respect to CH_4 by the equation:

$$\alpha = K_{CO_2}/K_{CH_4} \tag{2}$$

Membrane characterization

FTIR studies

Polyamide–polysulfone composite layer of the TFC membrane was peeled off from the nonwoven support fabric and FTIR spectra were scanned between 4000 and 400 cm^{-1} using Perkin-Elmer-283B FTIR spectrophotometer (Boston, MA, USA).

XRD analysis

A Siemens D 5000 powder X-ray diffractometer (NJ, USA) was used to study the solid-state morphology of polyamide–polysulfone composite layer of the TFC membrane. X-rays of 1.5406×10^{-10} m wavelengths were generated by a CuK-α source. Applying a scan rate of 0.06°/s, the angle (2θ) of diffraction was varied from 0° to 65° to identify the crystal structure and intermolecular distances between intersegmental chains. However, the study did not involve the usage of aluminum supports. Only the nonwoven fabric, which formed the bottom layer was peeled off before the X-ray analysis. The thicker polysulfone layer (45–50 μm) ensured that polyamide skin layer produced patterns when exposed to X-ray beam without the usage of external support material.

DSC studies

DSC thermogram of the TFC polyamide membrane was recorded on a Mettler Toledo 821^e instrument (Columbus, OH, USA) in the temperature range of 25–600 °C at the heating rate of 10 °C/min in nitrogen atmosphere.

Scanning electron microscopy

Surface and cross-sectional morphologies of polysulfone substrate and TFC polyamide membrane were taken using Hitachi S2150 scanning electron microscope (Ibaraki, Japan).

Estimation of cohesive energy density (CED) and solubility parameter (δ) of polyamide

Molecular simulations were performed on polyamide polymer using the MS modeling 3.1 software procured from Accelrys, San Diego, USA [26]. The simulation protocol includes molecular mechanics (MM) and molecular dynamics (MD) calculations. MD was performed using the COMPASS (condensed-phase optimized molecular potentials for atomistic simulation studies) forcefield [27]. The minimization was performed using the steepest descent approach followed by the conjugate gradient method. Temperature in all the simulations was equilibrated with the Andersen algorithm [28]. The velocity verlet algorithm [29] was then used to integrate the equations of motion. The group-based cut-offs were used with the explicit atom sums being calculated to 9.5×10^{-10} m. The tail correction was applied to the non-bonded interactions during the MD run. The oligomer chain was generated with 10 monomer units. It was minimized and the amorphous cells were constructed based on the respective densities of the selected oligomers. Details of the construction of amorphous cell module were reported earlier [30]. MD simulations under constant volume and temperature (NVT) ensemble were performed using the Discover program. Systems built with 3D periodicity were equilibrated in the NVT ensemble at 25 °C. Molecular dynamics run for 10 pico-seconds (ps) were performed to remove the unfavorable local minima that had high energies. Subsequently, systems were subjected to 200 ps of dynamics with trajectories being saved every 0.1 ps during the last half of the run to calculate the physical properties of interest.

Estimation of interaction energies

MD simulations were performed to estimate the interaction energies between polymers and the chosen gas molecules. The oligomer chain of polyamide polymer was generated and constructed as mentioned earlier. Polyamide oligomeric slabs were constructed using the confined layer (cell type) dialog in the amorphous builder. As a part of the amorphous cell construction, a geometry refinement of the structure was performed. Further, 2D boxes were built using the algorithm; then, polyamide as well as the selected gas molecule slabs was piled up and the box was extended by 100×10^{-10} m in the *c*-direction. In order to pile the cells correctly, gas layers (for 50 molecules of gas layer) were selected with the same base to be compatible with those of polyamide. MD simulations were run in the NVT ensemble at 25 °C with the tail correction being applied outside the cutoff of 9.5×10^{-10} m. This ensured that a relatively thin layer would feel the effective pressure equivalent to that in the bulk. Systems were then allowed to equilibrate normally against vacuum for approximately 30,000 steps. This was followed by 300 ps of the MD run. For every 500 femto-seconds (fs), the energy of interaction between oligomers and gas layer was evaluated using 18×10^{-10} m cut-off distance without the tail correction. A total of 600 energy calculations were performed for each system with 300 ps being the total simulation time.

Results and discussion

Membrane characterization

FTIR studies

Since polyamide skin layer was difficult to peel off from the substrate, FTIR spectra of the entire polyamide–polysulfone composite was taken (see Fig. 4), which revealed the bands that are ascribable to both the layers, since the beam penetration depth exceeds the thickness of the polyamide skin layer. FTIR assignments of the plain polysulfone [31] and polysulfone–polyamide composite are compared in Table 1 [6]. The band at 1638 cm^{-1} is ascribed to amide I (C=O stretch), while that at 1578 cm^{-1} is due to amide II (C–N stretch), which confirms the formation of polyamide. These bands are clearly distinguishable from the polysulfone FTIR bands.

From Table 1, it can also be inferred that the signal intensities are stronger for TFC composite (absorbance of

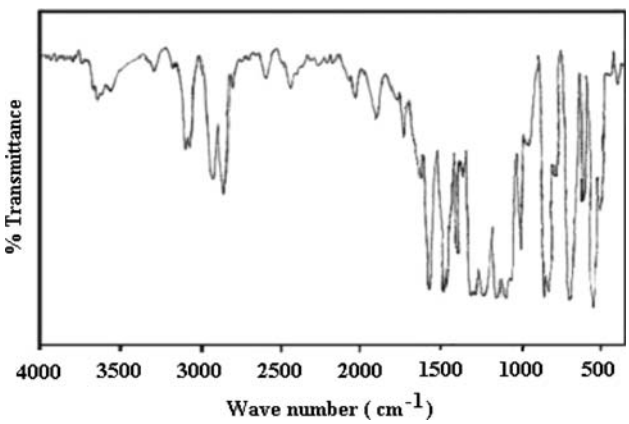

Fig. 4 FTIR spectrum of TFC polyamide membrane

Table 1 FTIR spectral assignments for polysulfone and polyamide–polysulfone composite

Spectral assignments	Frequency (cm^{-1})	
	Polysulfone	TFC polyamide
O–H aromatic stretching	3088	3096
O–H aliphatic stretching	2924, 2852	2926, 2855
C=O stretching (acid)	Nil	1734
C=O stretching (polyamide)	Nil	1638
C–N stretching (polyamide)	1368	1578
CH_3–C–CH_3 (symmetric deformation)	1368	1368
S=O stretching	1295	1295
C–SO_2–C (asymmetric stretching)	1320	1322

amide I is 0.019) due to the presence of large void space within the penetration depth of FTIR beam, signaling the presence of large pores. The pores of polysulfone membrane present in TFC membrane presumably favor the effective penetration of diamine monomer by forming an absorbed layer of the aqueous solution and subsequently, the acid chloride reacts with the diamine monomer diffused into the absorbed aqueous layer, leading to the formation of polyamide inside the pore. The formation of a thin skin layer is also evident from the partial attenuation of polysulfone bands. If all the polysulfone pores are coated by polyamide and a thin skin layer is formed, then the possibility of attaining higher permeabilities without adversely affecting the selectivity exists.

X-ray diffraction studies

The microstructure of polyamide–polysulfone composite was studied using the X-ray diffractometer. Figure 5 shows the broad peaks around 9–10° of 2θ, indicating an average intermolecular distance of 7.8×10^{-10} m in the amorphous portion, besides relatively sharp semi-crystalline peaks centered around 18–20° of 2θ, which emphasize the semi-crystalline nature of the composite [32]. The presence of crystalline regions in the composite are attributed to the polyamide skin, whereas amorphous regions are due to polysulfone. In general, crystallinity in polymers tends to reduce both penetrant solubility and diffusivity, thereby reducing the permeance [14]. In the present case, since the nature of the membrane is semi-crystalline, one can expect a moderate selectivity without any significant loss in the permeance.

DSC studies

Thermal behavior of TFC polyamide composite samples was studied using DSC. The first heating traces were recorded and presented in Fig. 6. The polyamide–polysulfone composite exhibits a strong melting endotherm around 240 °C, which is due to the crystallites present in the composite sample. The occurrence of an additional peak at 390–410 °C can be explained by the formation of new crystalline domains. At the annealing temperature (130 °C), amorphous regions of the polymer chains would have enhanced the chain mobility such that reorientation of polymer chains could take place with the formation of new crystalline domains with restricted chain mobility [33].

SEM studies

Figure 7 shows the surfaces of (a) ultraporous polysulfone substrate and (b) TFC polyamide membrane. The cross-sectional view of TFC membrane is presented in Fig. 7(c). The surface view of TFC polyamide is uniform and appears nonporous, indicating the presence of a dense skin layer. The cross-sectional view of TFC polyamide clearly depicts different shades of color of two layers, indicating the composite nature of the membrane, but no defects can be observed in the skin layer. The thickness of the skin layer appears non-uniform, and is therefore not reported. Penetration of polyamide skin into the porous polysulfone

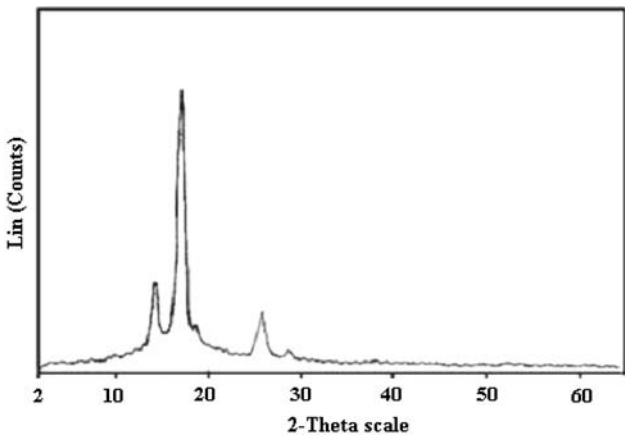

Fig. 5 XRD diffractogram of TFC polyamide membrane

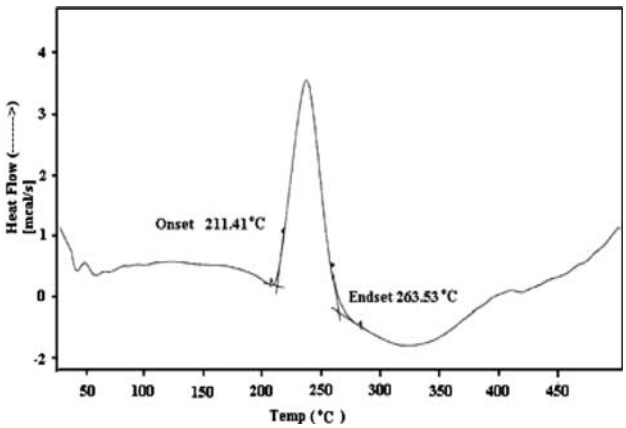

Fig. 6 DSC thermogram of TFC polyamide membrane

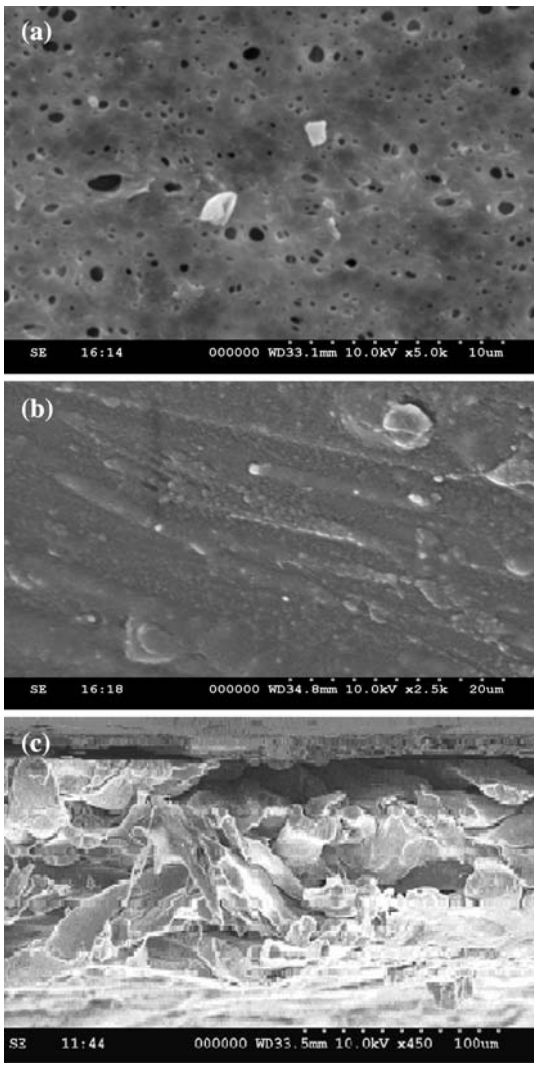

Fig. 7 SEM pictures representing (**a**) surface of polysulfone substrate, (**b**) surface of TFC polyamide membrane, (**c**) cross-section of TFC membrane

substrate can be observed. The permeance unit is used as a measure of gas transport property instead of permeability since the exact thickness cannot be determined.

Permeation results

It is a well-known fact that the performance of a membrane strongly depends upon the membrane preparation parameters such as solvent type, casting technique, annealing, etc. [34]. The present TFC polyamide membrane was subjected to annealing to reduce polymer swelling and prevent large increases in CO_2 diffusion coefficient at high feed pressures. Annealing at higher temperatures would result in the decrease of permeation rate [34] and hence, in the present study, a moderate temperature of 130 °C was used. Single gas studies were conducted on TFC polyamide membranes before and after annealing at a feed pressure of 1 MPa. The permeances and selectivities obtained are given in Table 2, wherein one can observe that annealing has resulted in an increase of selectivity of the TFC polyamide membrane without any significant loss in permeances. H_2S was found to be the fastest moving gas molecule with a permeance of 51.6 GPU for the annealed TFC polyamide, followed by CO_2 with a permeance of 15.2 GPU. The selectivity of 49.1 for H_2S/CH_4 was also highest, whereas that for CO_2/CH_4 was 14.4. H_2S and CO_2 are the soluble gases, which would undergo dissolution in the polyamide membrane that consists of polar -NHCO functional groups [35]. Hydrogen bonding interactions between these gases and amide groups of the membrane are expected to occur. On the other hand, CH_4 is relatively a saturated non-polar molecule, which showed minimum interaction with the membrane and subsequently, exhibited a low permeation rate. Diffusion coefficient of CO_2 is also higher than CH_4, since its kinetic diameter is 3.3×10^{-10} m as compared to 3.8×10^{-10} m for CH_4. Similarly, the corresponding kinetic diameter of O_2 is 3.46×10^{-10} m as compared to a value of 3.76×10^{-10} m for N_2. The selectivity of 5.4 for O_2/N_2 system appears to be reasonable based on the fact that published reports on other polymer membranes also exhibited a maximum selectivity of 6–8 for this system [35]. However, the selectivity values observed with single gases would lower when the membrane is exposed to binary feed gas mixtures due to enhancement of the permeance of the neutral gas such as CH_4 in the presence of more soluble gas such as CO_2 or H_2S [17].

Effect of feed pressure

TFC polyamide membrane was subjected to feed pressures varying from 1.0–3.0 MPa with three pure gases used in

Table 2 Permeation properties of various gases in TFC Polyamide membrane at 1 MPa

	Permeance (k) (GPU*)					Selectivity		
	CO_2	CH_4	H_2S	O_2	N_2	CO_2/CH_4	H_2S/CH_4	O_2/N_2
Before annealing	16.6	1.29	52.3	6.24	1.52	12.8	40.5	4.1
Post annealing	15.2	1.05	51.6	5.13	0.95	14.4	49.1	5.4

*1 GPU = 7.5×10^{-12} [$m^3/(m^2$ s Pa)]

this study. Figure 8 displays the effect of increasing pressure on permeation of CO_2/CH_4 and H_2S/CH_4 gas pairs, respectively. Figures 8 and 9 show an increase in permeances from 15.2 to 30.6 GPU for CO_2 and 1.05 to 1.68 GPU for CH_4, whereas the permeance of H_2S improved from 51.6 to 93.9 GPU. Thus, enhancement of the order of 101%, 80%, and 60% in CO_2, H_2S, and CH_4 permeances, respectively, are observed. Since natural gas is generally available at high pressures, a significant rise in CO_2 and H_2S permeances can be anticipated. However, at such high pressures, the high methane losses should also be considered and measures should be taken to prevent the excessive methane losses. However, these aspects are beyond the scope of this paper. From Fig. 9, a rise in H_2S/CH_4 selectivity from 49.1 to 55.9 can be evidenced. Similarly, a rise in CO_2/CH_4 selectivity from 14.4 to 18.2 was observed. A moderate increase in selectivity is possibly attributed to increased sorption of CO_2 and the polar H_2S gas molecules in the polyamide membrane. Literature suggests that sorption of the non-interacting CH_4 molecules remains almost the same as that of the inert N_2 gas [36]. Earlier, Sridhar and Khan [37] reported increased propylene sorption in ethyl cellulose membrane under similar operating conditions. A similar theory based on the solution-diffusion mechanism was also suggested [34] to explain the increasing separation trends of water from the salt molecules at increasing pressures, during desalination of water by reverse osmosis using TFC membrane. Figure 10 shows a more significant increase in O_2 permeance from 5.13 to 7.8 GPU than that of N_2 permeance; the latter showed only a marginal improvement from 0.95 to 1.23 GPU. Thus, enhancement of O_2 selectivity from 5.4 to 6.3 was observed.

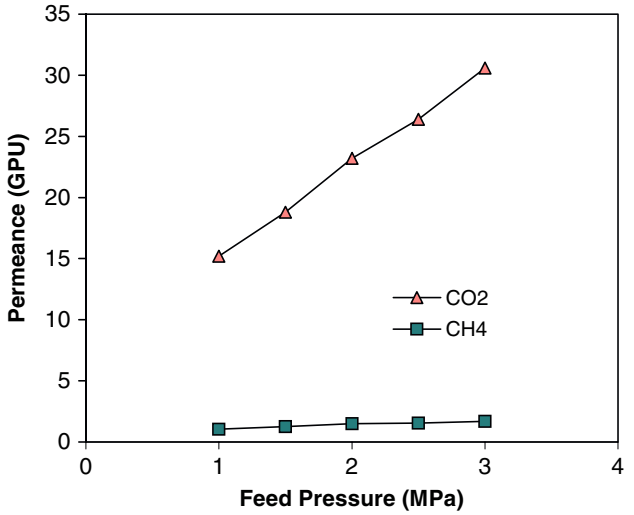

Fig. 8 Effect of feed pressure on permeation characteristics of pure CO_2 and CH_4 gases through TFC polyamide membrane

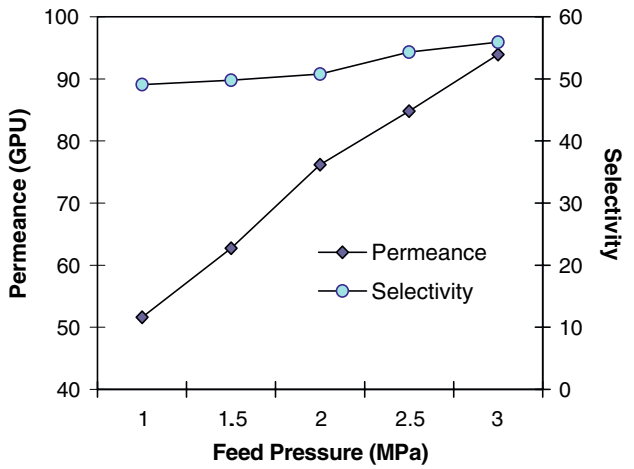

Fig. 9 Effect of feed pressure on H_2S permeability and H_2S/CH_4 selectivity through TFC polyamide membrane

Computation of CED and δ

Cohesive energy properties of the polymers are difficult to determine experimentally because the chosen polymers are insoluble, have high glass transition temperatures and are usually poorly characterized. Therefore, we thought of employing MD simulation techniques to obtain useful information of higher quality than other methods. We have performed a series of MD simulations to compute the CED of these polymers. In molecular simulation studies on polymers using the equation:

$$\text{CED} = (E_{coh}/V_{mol}) \tag{3}$$

CED is related to Hildebrand solubility parameter, δ through the equation:

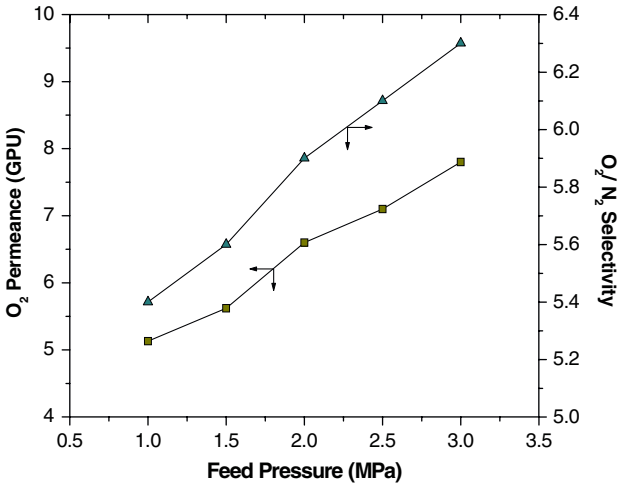

Fig. 10 Effect of feed pressure on O_2 permeability and O_2/N_2 selectivity through TFC polyamide membrane

$$\delta = \left(E_{coh} \Big/ V_{mol}\right)^{1/2} \quad (4)$$

In this context, computed *CED* and δ values of the selected polyamide are 173.1 J/m^3 and 13.16 (J/m^3)$^{1/2}$, respectively, which proves the accuracy of the estimations since the experimentally determined δ of polyamide was around 11.5 (J/m^3)$^{1/2}$ [30].

Interaction of polyamide with the chosen gas molecules

Sorption behavior of the polymers with CO_2, H_2S, CH_4, O_2, and N_2 was estimated using MD simulation protocols. A representative structure of polyamide with 50 N_2 gas molecules is displayed in Fig. 11. Interaction energy values of polyamide calculated for H_2S, CO_2, O_2, CH_4, and N_2 are, respectively, –228.43, –142.25, –97.44, –42.54, and –25.49 kJ/mol. The lower the energy required, the greater is the extent of interaction of the gas species with the membrane resulting in higher sorption. These trends support the permeation trends of the selected gases with polyamide membrane reported in Table 1, which show permeability to decrease in the same order of $H_2S > CO_2 > O_2 > CH_4 \approx N_2$. Thus, the simulated results are quite comparable with the experimental observations, suggesting the validity of the simulation protocols employed in this study.

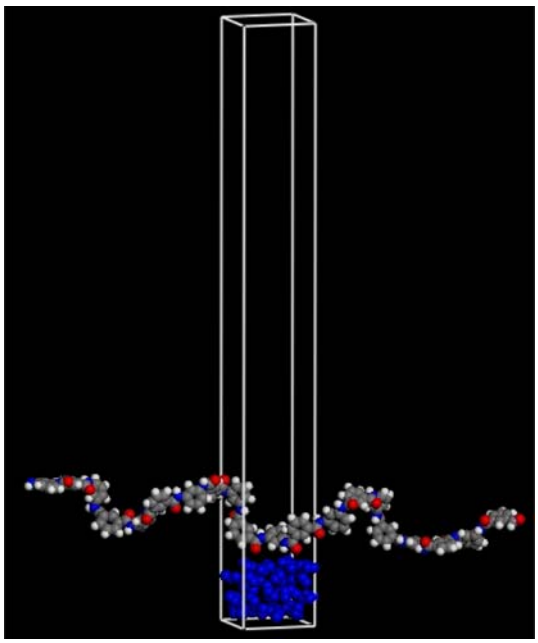

Fig. 11 A representative structure of polyamide interacting with 50 N_2 molecules (carbon atoms are gray, hydrogen-white, oxygen-red, N_2-blue)

Conclusions

The present invention is an effort to develop novel type of TFC polyamide membrane by interfacial polymerization to study its separation characteristics for CO_2/CH_4, H_2S/CH_4, and O_2/N_2 gaseous systems. It was realized that polyamide membranes may not generally offer an attractive balance of permeance and selectivity because of their high cohesive energy density. The present study, however, demonstrates the possibility to obtain a proper balance by preparing an ultrathin defect-free polyamide skin layer on a tight polysulfone substrate. Pore structure of the substrate was found to be quite crucial for the successful synthesis of TFC polyamide membrane that can be used in gas separation studies. The membrane exhibited a reasonable selectivity for CO_2/CH_4 system and a high selectivity for H_2S/CH_4 system. The difference in permeances of the gases validates that interfacial polymerization could be a useful route to fabricate efficient gas-separating membranes.

FTIR spectra revealed the presence of amide I and amide II peaks besides the sulfone groups of the polyamide–polysulfone composite. X-RD indicated the semi-crystalline nature of the membrane. DSC exhibited a strong melting endotherm around 220 °C. SEM showed that membrane surface was uniform with no visible pores, whereas cross-sectional view exhibited a polyamide skin on a porous polysulfone layer of different color shades. TFC polyamide membrane was found to be a promising candidate for deacidification of natural gas by exhibiting a high selectivity for H_2S and CO_2 acid gases over the major hydrocarbon constituent viz., methane. Sorption of CO_2 and H_2S was more pronounced with increasing feed pressure, which improved the permeance and selectivity with respect to CH_4. The O_2/N_2 selectivity was reasonably high. Further research in this area is in progress to improve the membrane selectivity using different reagents for interfacial polymerization or modification of the active skin layer. The permeability results obtained are in accordance with the theoretically evaluated values of interaction energies and solubility parameters of gas molecules in the polyamide membrane. Lower energies of interaction were observed in case of the more soluble H_2S, CO_2, and O_2 gases compared to the relatively inert N_2 and CH_4 gases. Computed CED and δ values of the selected polyamide membrane proved the accuracy of the molecular dynamics simulation method.

Fabrication and testing of a spirally wound TFC polyamide module will constitute our future course of action.

Acknowledgments Professor Aminabhavi MT thanks the University Grants Commission, New Delhi (Grant No. F1-41/2001/CPP-II) for a financial support to establish Center of Excellence in Polymer Science. Mr. S. Sridhar thanks Department of Scientific and Industrial

Research (DSIR), New Delhi, and EIL (Gurgaon) for their support during the course of this work.

References

1. Zhou Y, Yu S, Liu M, Chen H, Gao C (2006) Desalination 192:182
2. Verissimo S, Peinemann K-V, Bordado J (2005) J Membr Sci 264:48
3. Zhang Y, Xiao C, Liu E, Du Q, Wang X, Yu H (2006) Desalination 191:291
4. Wahab Mohammad A, Hilal N, Semana MNA (2003) Desalination 158:73
5. Verissimo S, Peinemann K-V, Bordado J (2005) Desalination 184:1
6. Lianchao L, Baoguo W, Huimin T, Tianlu C, Jiping X (2006) J Membr Sci 269:84
7. Kim HJ, Lee HK, Kim YS (2000) J Membr Sci 169:81
8. Ahmad LA, Ooi SB (2005) J Membr Sci 255:67
9. Roh JI, Greenberg AR, Khare PV (2006) Desalination 191:279
10. Prakash Rao A, Joshi VS, Trivedi JJ, Devmurari VC, Shah JV (2003) J Membr Sci 211:13
11. Yong Z, Sanchuan Y, Meihong L, Congjie G (2006) J Membr Sci 270:162
12. Zhang W, He G, Gao P, Chen G (2003) Sep Purif Tech 30:27
13. Koros WJ, Mahajan R (2000) J Membr Sci 175:181
14. Kesting ER, Fritzsche KA (eds) (1993) Polymeric gas separation membranes. Wiley, New York
15. Astarita G, Savage WD, Bisio A (eds) (1983) Gas treating with chemical solvents. John Wiley & Sons, Inc., New York
16. Kohl LA, Riesenfeld CF (eds) (1974) Gas purification, 2nd edn. Gulf Publishing Co., Texas
17. Koros JW, Fleming KG (1993) J Membr Sci 83:1
18. Hao J, Rice AP, Stern AS (2002) J Membr Sci 209:177
19. Espeso J, Lozano EA, De La Campa JG, De Abajo J (2006) J Membr Sci 280:659
20. Ekiner MO, Vassilatos G (1990) J Membr Sci 53:259
21. Petersen J, Peinemann K-V (1997) J Appl Polym Sci 63:1557
22. De Abajo J, De La Campa JG, Lozano EA, Espeso J, Garcia C (2003) Macromol Symp 199:293
23. Ulbricht M (2006) Polymer 47:2217
24. Koros JW, Pinnau I (1994) In: Paul RD, Yampol'skii YP (eds) Polymeric gas separation membranes. CRC Press, Boca Raton, Florida, USA
25. Sridhar S, Smitha B, Ramakrishna M, Aminabhavi TM (2006) J Membr Sci 280:202
26. Accelrys Inc. MS Modeling, Accelrys Inc., San Diego, CA, 2003
27. Sun H (1998) J Phys Chem B 102:7338
28. Andersen HC (1980) J Chem Phys 72:2384
29. Verlet L (1967) Phys Rev 159:98
30. Prathab B, Aminabhavi TM, Parathasarathi R, Manikandan P, Subramanian V (2006) Polymer 47:6914
31. Smitha B, Sridhar S, Khan AA (2003) J Membr Sci 225:63
32. Kang YS, Lee S, Kim YU, Shim SJ (1990) J Membr Sci 51:215
33. Singh SP, Joshi VS, Trivedi JJ, Devmurari VC, Prakash Rao A, Ghosh KP (2006) J Membr Sci 278:19
34. Hacarlioglu P (2001) Effect of preparation parameters on performance of dense homogenous polycarbonate and polypyrrole–polycarbonate mixed matrix membranes. MS Thesis, Middle East Technical University, Ankara, Turkey
35. Ho WSW, Sirkar KK (eds) (1992) Membrane handbook. Van Nostrand Reinhold, New York
36. Stern AS (1994) J Membr Sci 94:1
37. Sridhar S, Khan AA (1999) J Membr Sci 159:209